Chapter 5:

SEISMIC HAZARDS AND STATIC STRESS

Chapter 5:

Seismic hazard assessment and static stress estimation in and around the source zone of past major earthquakes of Northwestern Himalaya, India

5.1. Introduction

In the previous chapter, the seismicity and the tectonic processes was carried out to infer the different slip potentials and how seismicity is controlling the tectonics of present region. However, it is also important to study the hazards and the stress developing in the area due to intense seismicity. Hence, in this chapter, the current seismic stress pattern scenario in the NW Himalaya and the associated hazard are studied. The static stress change due to the past four major earthquakes namely the 1905 Kangra earthquake, 1975 Kinnaur earthquake, 1991 Uttarkashi earthquake and 1999 Chamoli earthquake that occurred in NW Himalaya, India are studied utilizing the Coulomb 3.1 application. Coulomb stress change is calculated utilizing the presumed three factors. 1905 Kangra earthquake shows a maximum stress associated with the MHT detachment and some of the previously shadow zone has been reactivated. For the 1975 Kinnaur earthquake it is observed that there is a reactivation of the previously seismic shadow zone. For 1991 Uttarkashi earthquake the high seismic stress is observed over the lesser and Higher Himalaya and major structural discontinuities like MBT and MCT both getting activated and triggering aftershocks. In case of 1999 Chamoli earthquake a significant stress shadow is observed in some parts of the lesser Himalaya and a significant high stress is noted on the rest part of the NW Himalaya. All the above results shows that the tectonic stress in NW Himalaya is quite high and the region is near to failure chancing major earthquakes in future.

Himalaya is undergoing maximum compression due to the convergence of the India and the Eurasian plate since 55 Ma. As a result of

this convergence, the Northwest (NW) Himalayan segment extending between a latitude and longitude range of 30°N to 33°N and 76°E to 80°E experienced four most deadliest earthquakes. They may be listed as 1905 Kangra earthquake (Ms = 7.8) (Middlemiss, 1910; Mathur, 1953; Poddar, 1953),1975 Kinnaur earthquake (Ms = 6.8) (Khattri et al., 1978), 1991 Uttarkashi earthquake (Ms = 6.8) (Cotton et al., 1996) and 1999 Chamoli earthquake (Ms = 6.6) (Kayal et al., 2003). The spatial distribution and the types of faulting mechanism of these earthquakes in an active tectonic regime like the Himalaya help us to understand the physical processes which control the ongoing tectonic activity in the region. In past, a large number of studies have been carried out in Himalaya (Seeber and Armbruster, 1981; Ni and Barzangi, 1984; Chander, 1988; Molnar 1990) and these studies further conclude that the great earthquakes occurs on a major north dipping detachment fault called as the Main Himalayan Thrust fault (MHT). The occurrence of four great earthquakes in a narrow acute Himalayan arc within a short span of 50 years itself explains the vulnerability of the arc from seismic hazard point of view. Again from seismotectonic view point the NW Himalaya has frequently experienced major earthquakes having a magnitude ($Mw \geq 6.0$) in the recent past. Therefore the critical analysis of these moderate earthquakes along with their aftershocks distribution and occurrences is necessary to provide implications for the seismic hazard assessment of the region. Here in this study, the theory of Coulomb failure function (CFF) is applied to study the four moderate to strong earthquakes occurred in the region. It may be noted that when the stress in a particular feature like rocks increases beyond a particular limit called the critical stress then it gives rise to fractures and deformations within it. This increase in stress due to major earthquakes can lead to a large triggering of aftershocks that follow the main shock in the nearby region of critical failure (Smith and Van de Lindt 1969; Hamilton 1972; Rybicki 1973; Yamashina 1978; Das and Scholz 1982). Thus studying the static stress changes based on Coulomb stress transfer model helps in understanding the direction of propagation of the seismic events in that region.

This theory has been successfully applied to study many large earthquakes and is found to produce good results (Harris 1998). In our present

analysis the Coulomb stress transfer model is applied to three moderate to strong earthquakes (viz. Kinnaur earthquake (1975); Uttarkashi earthquake (1991); and the Chamoli earthquake (1999)) to find out the correlation between the static stress change and the earthquake occurrence in the NW Himalaya. As reported from previously carried out earthquake studies in the region it can be concluded that in recent past there has been an enormous increase in the seismic activity due to tectonic stress perturbations in the NW Himalaya. Through this analysis,it is able to find out whether this increase seismicity has any linkage with the Himalayan major fault system or it may be associated with the shadow of past earthquake in NW Himalaya region. This study is particularly carried out based on the Coulomb stress model. The static stress changes and the triggering of earthquakes in the region have been studied under the three principal assumptions. They may be listed as follows:

1) The earthquake source to be acting as a receiver fault.
2) Recent earthquakes occurring in the aftershock zone of the major earthquakes acting as receiver for the source earthquake.
3) Receiver as a major fault system of Himalaya where no much seismicity is reported.

The study is carried out in a region falling between latitude ranges of 30°N to 33°N and a longitude range of 76°E to 80°E. The total encompassed area is further divided in to 0.05° × 0.05° grids and it is assumed that the coulomb stress change on every point lying inside the grid is same throughout. Coulomb 3.1 (Toda et al. 2007), a graphic rich deformation and stress change software, is used to generate the grids and study the static stress change. The coulomb estimation software (Toda et al. 2007) needs an input file with all required information to calculate the static stress change for the study region. So first of all an input file with latitude, longitude of the study area is built and all the information's pertaining to the earthquake source and receiver fault is provided in it. The source mechanisms of the main shocks are adopted from USGS, NEIC and ISC catalogue for major source earthquakes. The aftershocks of the major earthquakes with the region are computed up to December 2013. Again the stress state of the regional tectonic faults is studied

to understand the effects of the main shocks. Some recent earthquakes recorded and determined from our previous studies as discussed in earlier chapter are used to study the correlation between the main shocks and its occurrence. These major aftershocks are seen to fall in a high stress region of the major main shocks of the NW Himalaya. The present validates the facts that still the region is under the high stress regime due to major past earthquakes. This can be a significant warning or prediction that may be these small earthquakes can be pertained to a coming great earthquake in the region. As our findings validate that the stress perturbation in the study region can trigger major earthquakes in future. The aftershocks are studied in order to delineate the stress propagation in the region that can lead to a number of earthquakes in the nearby region in future.

5.2. Modeling Coulomb failure static stress changes

Stress change on the seismogenic faults in tectonically disturbed regions can cause damaging earthquakes in the region. Thus the study is set to calculate the present day stress change due to tectonic loading or fault interactions can be useful in predicting future earthquakes. In this regard the calculated change in Coulomb failure stress (ΔCFS) caused by an earthquake is given by equation

$$\Delta CFS = \Delta\tau - \mu' (\Delta\sigma n) \quad (5.1)$$

where, $\Delta\tau$ is the change in shear stress calculated on the orientation and kinematics of either optimally oriented faults, or of specified faults, μ' is the coefficient of effective friction, and $\Delta\sigma n$ is the change in normal stress. Coulomb stress change have been widely applied to study the interaction between various earthquakes since the 1980's (e.g., King et al., 1994; Stein et al., 1997; Harris, 1998; Stein, 1999; Parsons et al., 2000; Toda et al., 2008).

The ultimate failure of the rocks on the considered or occurred faults is associated with positive resulted positive ΔCFS and that associated with a negative ΔCFS will result in a delayed failure on those fault planes. The regions placed under the positive ΔCFS is categorised under the high stress

regime and the vice versa is placed under the low or stress shadow category. Here in the present study, only the co-seismic (time-independent) Coulomb stress changes have been calculated. The fault interactions resulted in to a simultaneous change of both shear stress (τ) and normal stress (σn) along with earthquake occurrences so it is termed as the static Coulomb stress change as co-seismic Coulomb stress changes. The determination of co-seismic Coulomb stress changes requires the estimation of stress changes on targeted source and receiver faults in terms of change in slip, creeps and displacements on them. The static stress change determined on targeted fault planes is associated with the crustal displacement (Gupta et al., 2015). Thus the static stress change can either accelerate or delay the occurrence of earthquake on the fault depending on the increase or decrease of static stress on the fault (Stein et al., 1997; Zhang et al., 2001). A different approach to study three strong earthquakes namely the 1975 Kinnaur earthquake, 1991 Uttarkashi earthquake and the 1999 Chamoli earthquake that occurred in the NW Himalaya, India in the past are presented. The qualitative analysis of these significant earthquakes can result in understanding the current seismic risk associated with the region due to these earthquakes and their aftershocks in spatial and temporal distributions. The co-seismic ΔCFS using the elastic half-space based software Coulomb 3.3 (Toda et al., 2011) are computed. For the computation of the Coulomb static stress change an input file is needed containing all information's (for e.g., location, size, fault parameters for source and targeted receiver faults, frictional coefficient and rheological parameters). There are generally two kinds of input files they may be stated as (.inp) and (.inr) files where (.inp) are attributed to source slip by right-lateral and reverse slip by left-lateral. Since, there is no slip model for the earthquakes the (.inr) input files was used. The (.inr) input format specifies rake (°) and net slip, which permits one to calculate the stress change on receivers (faults without slip) in their rake directions, where, for example, a left-lat. stress increase would inhibit failure on a right-lateral fault. A basic map with the low and upper bound latitude/longitude information of the study area for the respective earthquakes is built. The location, size and the fault plane parameters for the respective studied earthquakes are provided as input.

The rupture parameters (rupture length and rupture width) for the seismic events are computed using the empirical relation of Wells and Coppersmith, 1994. After building the input file this file is saved and called for static Coulomb stress computation for respective earthquakes. The static coulomb stress was finally computed by following the three above mentioned criteria's. They may be stated below as:

1) The earthquake source to be acting as a receiver fault.
2) Recent earthquakes occurring in the aftershock zone of the major earthquakes acting as receiver for the source earthquake.
3) Receiver as a major fault system of Himalaya where no much seismicity is reported.

In this way the static ΔCFS is computed for the three significant earthquakes i.e. 1975 Kinnaur earthquake; 1991 Uttarkashi earthquake; 1999 Chamoli earthquake using the above mentioned criteria.

5.3. Fault geometry, frictional-coefficient and depth of computation for specific earthquakes

The geometry and the kinematics of source and the targeted receiver faults need to be known before computing the Coulomb stress modelling. The earthquakes in this study have been widely recorded with a number of reporting agencies such as USGS, ISC-EHB so we have easily deduced the parameters with reasonable degree of detail. The average slip is assessed for a given earthquake using empirical relationships among event magnitude, rupture length, width, area and surface displacement (e.g. Wells and Coppersmith, 1994). In this regard the receiver faults have been different for different earthquakes. Like for the Kinnaur earthquake the Kaurik-Chango fault have been regarded as the targeted receiver fault. The Strike, Dip and Slip for the same have been adopted from the previously reported results in Bhargava et al., 1978. Similarly for the recent earthquakes acting as a receiver fault the determined fault parameters from previously reported studies in Chapter 4 as provided in Table 4.3 have been used. Similarly the main Himalayan detachment (MHT) acting as a receiver for some earthquakes in

particular for the 1991 Uttarkashi earthquake and the 1999 Chamoli earthquake the parameters have been considered from the previous reported results in the study area by Molnar 1990. The frictional-coefficient for all the earthquakes for which the static ΔCFS is computed is considered to be of 0.40 which is regarded as a moderate frictional coefficient for unknown faults.

5.4. Stress pattern scenario in NW Himalaya

5.4.1. 1905 Kangra earthquake

The 1905 Kangra earthquake of magnitude Mw 7.8 is regarded as one of the most deadly of the Himalayan earthquakes to occur in the western Himalaya, India region. This earthquake killed almost 20, 000 people and accounted for the damage of 100,000 buildings (Sharma and Lindholm 2011).The ground shaking due to this earthquake was felt extensively all over India, and intensities of the order of X on MMI scale were observed in most of the areas near the source (Ghosh and Mahajan 2013). The epicentral location of the April 4 1905 seismic event is considered to be 32.30N: 76.50E (ISS source) and the depth to the source is considered to be 18 km (Wallace et al., 2005). The Kangra-Chamba region is marked with the presence of nappe structure called distinctly as Chamba Nappe (CN) (Thakur 1992). This nappe comprises of the weakly metamorphosed sediments resulted due to south-westwards sliding of the Tethyan Himalayan Sequence (THS) from thenorth over the metamorphic Higher Himalayan Crystallines (HHC) along the south-dippingChenab Normal Fault (CNF) that separates the CN from the HHC (Thakur 1992; Kumaret al. 2009). This region is also characterised with the presence of some of the significant local tectonic breaks such as Jwalamukhi Thrust (JMT), Barsar Thrust (BT) and Palampur Thrust (PMT); thus, the MBT is not a single entity, rather than denoted as MBTs (Thakur 1992, 1998; Singh 1994). Since past decades this region which marks the southern edge of the Tibetan plateau has been hit by moderated earthquakes, and till now no earthquake has ruptured the Himalayan frontal Thrust (HFT) bounding the Himalayan foothills (Ambraseys and Bilham 2000; Kumar and Mahajan 2001; Kumar et al. 2001; Bilham 2001). Therefore this region can also be regarded as one of the most sensitive vulnerable regions of the western Himalaya in

terms of current and future seismic hazard assessment. The present study conceived for the reassessment of the 1905 Kangra earthquake zone in terms of static stress condition for future earthquake hazard point of view. In the present study, the coulomb stress associated with the April 4 1905 earthquake is computed following the presumed three conditions stated above for static stress estimation. Focal mechanism solutions reported for the earthquake by Wallace et al., 2005 for this earthquake constrained to a strike value of 135°N, dip of 7° are utilized for static coulomb stress computation. The length and width for the rupture is considered to be approximately 100×55 km adopted from Wallace et al., 2005. At first the static ΔCFS at the source of the 1905 Kangra earthquake with the source acting as the major receiver is computed. It can be seen from the computation for this earthquake that the rupture is propagating along the strike of major tectonic breaks in the region in a NNW–SSW direction. The major structural trends such as Main Boundary Thrust (MBT) and Main Central Thrust (MCT) falls under high stress zone presiding to the occurrence of this major seismic event. Some major local scaling structures such as Jwalamukhi Thrust (JMT) and Sundarnager Fault (SNF) also signify a major high static stress due to the earthquake. More number of aftershocks and current seismicity is reported in these major stress high zones. Another important feature that is observed in the current study is the frontal part of the Himalaya bounded with the Himalayan Frontal Thrust (HFT) which comes under stress shadow zone. It means the non-rupture of the frontal zone lying in the Himalayan foothills is justified due to the occurrence of this major earthquake event of 1905. The South Tibetan Detachment fault (STD) also comes under the stress shadow zone. The static ΔCFS at up dip depth of 20 Km with the frictional-coefficient (μ) of 0.40 is computed. As most of the aftershocks are having a depth of ~ 20 Km hence it is computed at this depth.

The *Figure 5.1* clearly demonstrates the high and low stress values over the region due to the occurrence of the 1905 Kangra earthquake. Four recently recorded earthquakes in the period from 2012 to 2013 in the epicentral zone of this major western Himalaya seismic event having a magnitude distribution (Mw 4.0 to 4.9) is also shown. The source parameters for all these seismic events are shown below:

Event date (DAMOYR)	Origin Time (UTTC)	Lat. (°N)	Long (°E)	Depth (km)	Mag. (Mw)	Strike	Dip	Rake	Strike	Dip	Rake
04.06.2013	17:34:50	32.672	76.601	28	4.9	294	27	-92	117	63	-89
05.06.2013	22:04:03	32.907	76.286	47	4	250	16	26	78	89	132
13.07.2013	17:49:36	32.383	76.535	5	4.4	323	15	15	128	75	-94
29.08.2013	10:13:24	31.479	76.273	47	4.4	78	89	89	78	89	132

Table 5.1. Source parameters of recent earthquakes in the epicentral zone of 1905 Kangra earthquake estimated utilizing the waveform inversion approach.

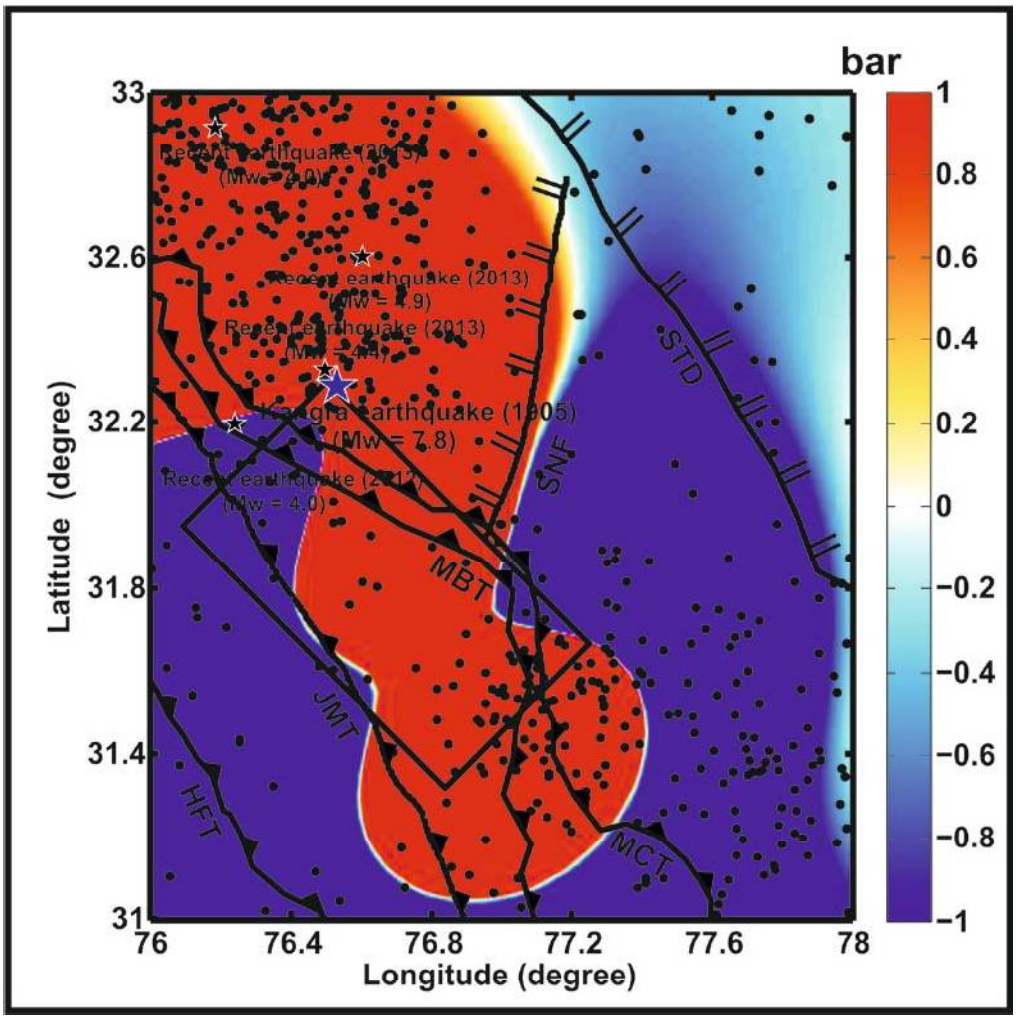

Figure 5.1: clearly demonstrates the high and low stress values over the region due to the occurrence of the 1905 Kangra earthquake. Four recently recorded earthquakes in the period from 2012 to 2013 in the epicentral zone of this major western Himalaya seismic event having a magnitude distribution (Mw 4.0 to 4.9) is also shown.

In the next step the recent recorded Mw = 4.0 event of 11.11.2012 as the major receiver fault for the 1905 Kangra earthquake are considered. The source parameters are considered as 280° N strike, 24° dip and -105° rake. The static ΔCFS at up dip depth of 20 Km with the frictional-coefficient (μ) of 0.40 has been computed. It is observed in this case that this epicentral zone of 11.11.2012 Mw = 4.0 event is under stress shadow and now recently seem to have been reactivated. The stress propagation is along NW-SE as well as E–W

direction accounting for both strike parallel and perpendicular rupture propagations in *Figure 5.2*.

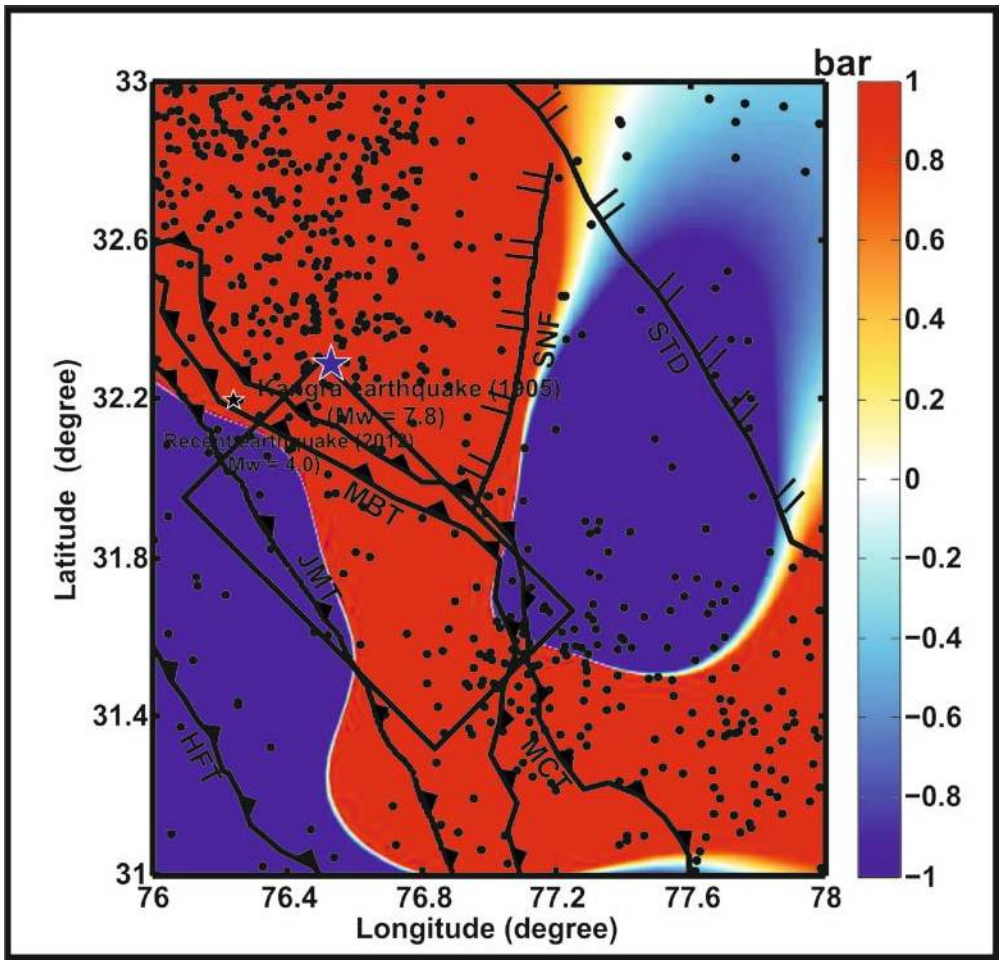

Figure 5.2: clearly demonstrates the high and low stress values over the region due to the occurrence of the 1905 Kangra earthquake with the epicenter of the recent recorded Mw 4.0 earthquake event.

The next computation consider the recent recorded Mw = 4.9 event of 04.06.2013 as the major receiver fault for the 1905 Kangra earthquake. The source parameters are considered as 294° N strike, 27° dip and -92° rake. The static ΔCFS at up dip depth of 20 Km with the frictional-coefficient (μ) of 0.40 have been computed. Again it is observed in this case that this epicentral zone of 04.06.2013 Mw = 4.9 event is under same high stress as it seems to be after the 1905 Kangra seismic event. The stress propagation is along NW–SE

along the same rupture zone of the 1905 Kangra earthquake. The major distinction to this computation is that the Jwalamukhi Thrust (JMT) which act as a major receiver for the 1905 Kangra earthquake is falling under the stress shadow zone and it consists of lesser number of aftershocks as the major aftershocks are distributed under the high stress zone lying in the NW and SE region of the 1905 Kangra rupture as designated in *Figure 5.3*.

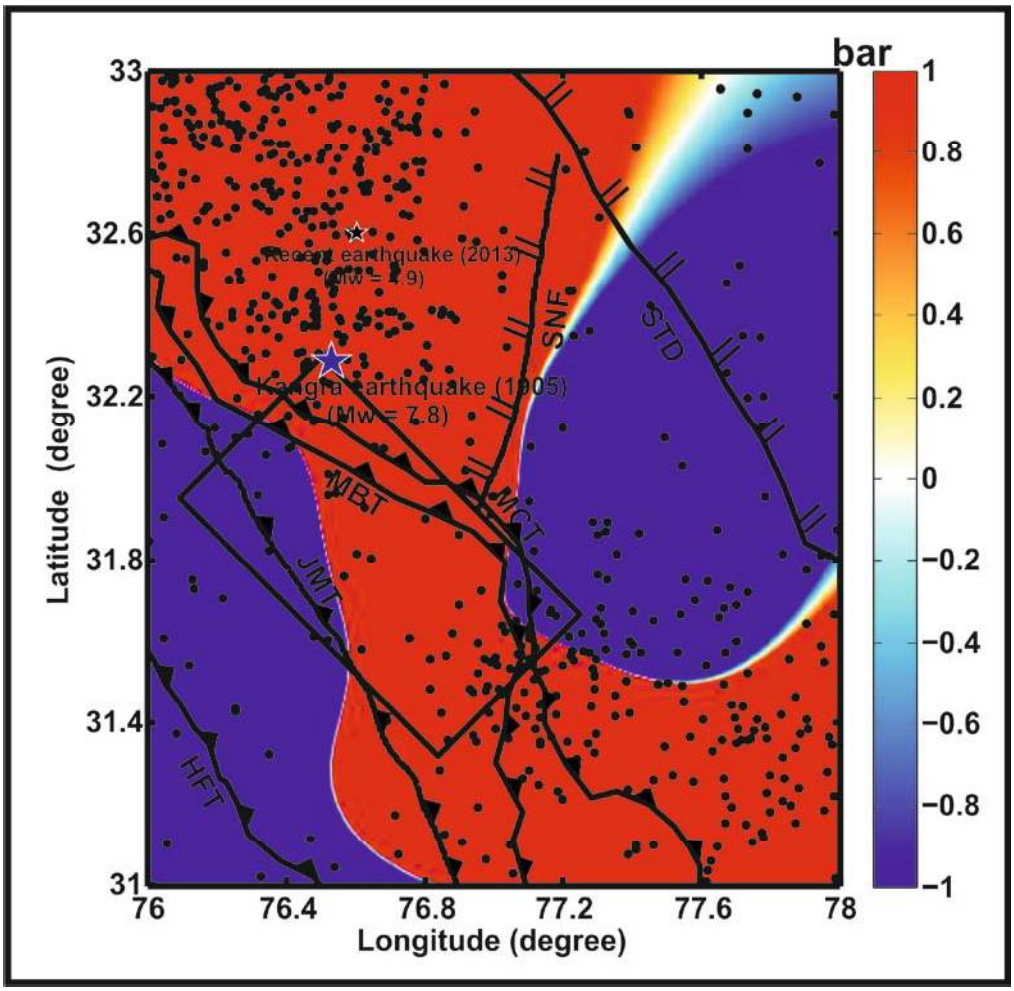

Figure 5.3: clearly demonstrates the high and low stress values over the region due to the occurrence of the 1905 Kangra earthquake with the epicenter of the recent recorded Mw 4.9 earthquake event.

Following the same presumed factors for the recent earthquakes acting as major receivers for the 1905 Kangra earthquake the static ΔCFS for the recent recorded Mw = 4.0 event of 05.06.2013 as the major receiver fault for

the 1905 Kangra earthquake is computed. The source parameters are considered as 250° N strike, 16° dip and 26° rake. The static ΔCFS at up dip depth of 20 Km with the frictional-coefficient (μ) of 0.40 is computed. The main observations in this case is that this epicentral zone of 05.06.2013 Mw = 4.9 event and this event has resulted a stress shadow over the majority of the Jwalamukhi Thrust (JMT) that act as a major receiver for the 1905 Kangra earthquake and for the time being the Himalayan Frontal Thrust (HFT) falls under the high stress zone. The stress propagation is along NW–SE along the same rupture zone of the 1905 Kangra earthquake. The major distinction to this computation is that the Jwalamukhi Thrust (JMT) act as a major receiver for the 1905 Kangra earthquake which is falling under the stress shadow zone and consists of lesser number of aftershocks as the major aftershocks are distributed under the high stress zone lying in the NW region as clearly pictured in *Figure 5.4* .

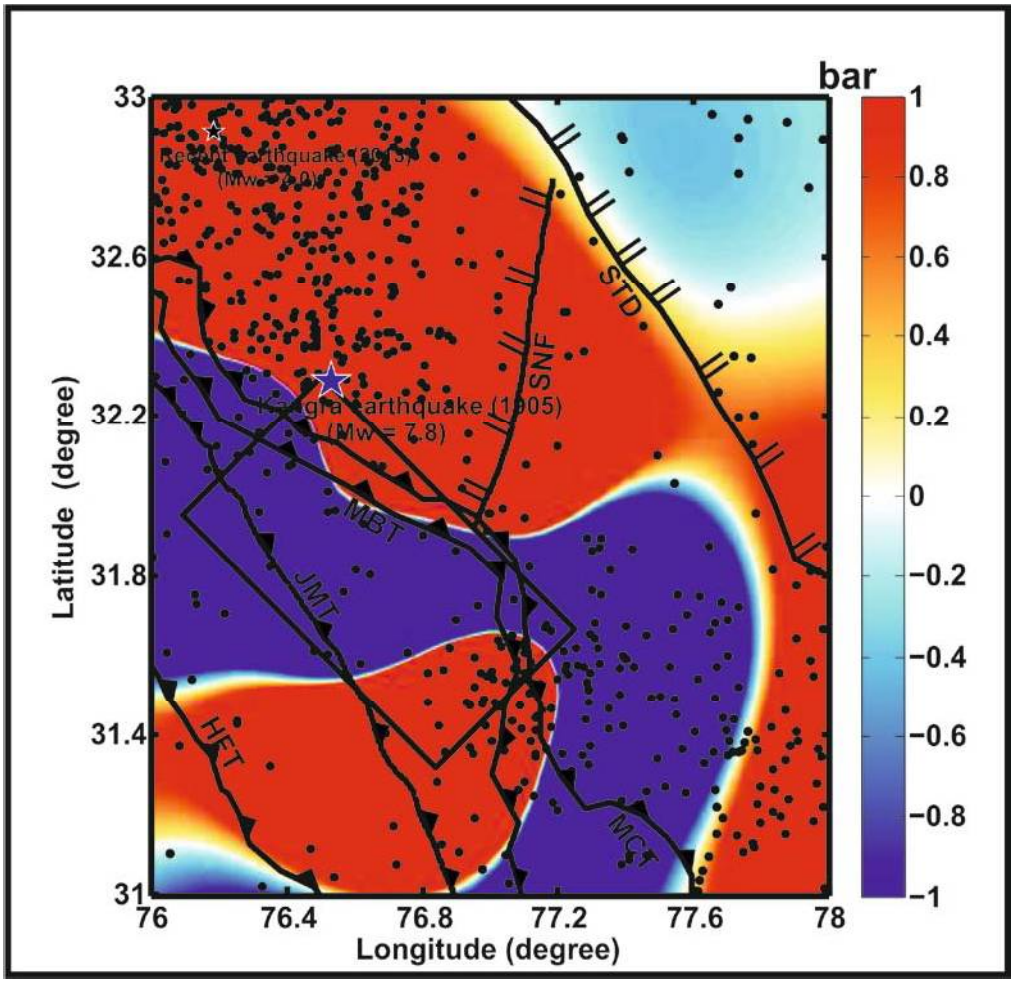

Figure 5.4: clearly demonstrates the high and low stress values over the region due to the occurrence of the 1905 Kangra earthquake with the epicenter of the recent recorded Mw 4.0 earthquake event.

The next work constrained to the recent earthquakes acting as a major receivers for the 1905 Kangra earthquake which is computed based on the static ΔCFS for the recent recorded Mw = 4.4 event of 13.07.2013 which is acting as the major receiver fault for the 1905 Kangra earthquake. This computation for static stress in the same epicentral zone of the 1905 Kangra earthquake is carried out following the same presumed factors adopted for other recently recorded events in the epicentral zone. The source parameters are considered are 323° N strike, 15° dip and 15° rake. The static ΔCFS at up dip depth of 20 Km with the frictional-coefficient (μ) of 0.40 is computed. The observations regarding the stress condition prevailing in the epicentral zone of the 13.07.2013 Mw = 4.4 event is likely to instigate that again a significant low stress or stress shadow is observed over the Himalayan Frontal Thrust (HFT) and a significant high stress is observed over the Jwalamukhi Thrust (JMT). The stress propagation is along NW–SE along the same rupture zone of the 1905 Kangra earthquake as shown in *Figure 5.5*.

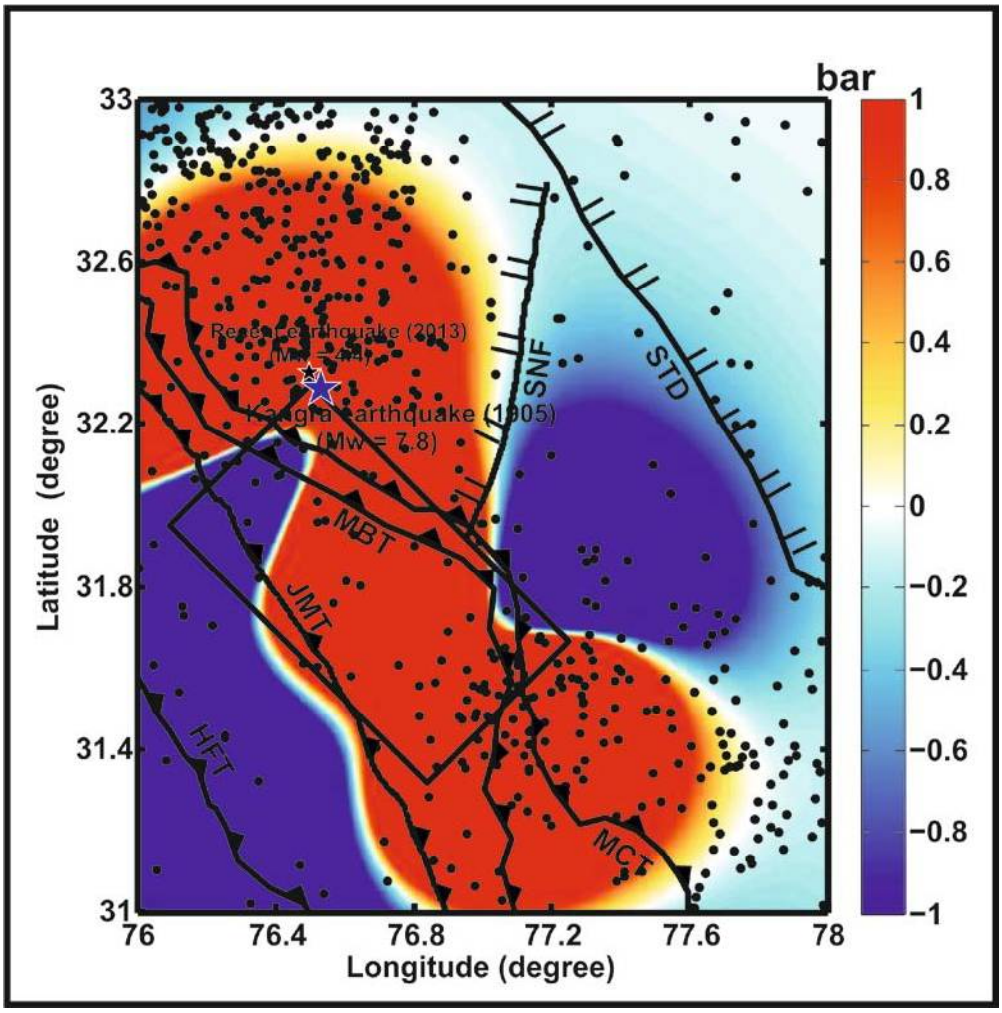

Figure 5.5: clearly demonstrates the high and low stress values over the region due to the occurrence of the 1905 Kangra earthquake with the epicenter of the recent recorded Mw 4.4 earthquake event.

The next work carried out signifying the Himalayan detachment acting as major receiver for the 1905 Kangra earthquake. The static ΔCFS for the major structural trends Main Boundary Thrust (MBT), Main Central Thrust (MCT), Himalayan Frontal Thrust (HFT) combined in the form of MHT detachment based on the previously mentioned conditions is computed. The source parameters are considered for computation are 280° N strike, 15° dip and 90° rake for the MHT detachment acting as a major receiver for the 1905 Kangra earthquake.

The static ΔCFS at up dip depth of 20 Km with the frictional-

coefficient (μ) of 0.40 has been computed. The observations regarding the stress condition prevailing in the epicentral zone of the 1905 Kangra earthquake of Mw = 7.8 event is likely to instigate that again a significant low stress or stress shadow is observed over the Himalayan Frontal Thrust (HFT) and a significant high stress is observed over the entire Himalayan detachment or the Main Himalayan Thrust. The stress propagation is along NW–SE along the same rupture zone of the 1905 Kangra earthquake is shown in *Figure 5.6*.

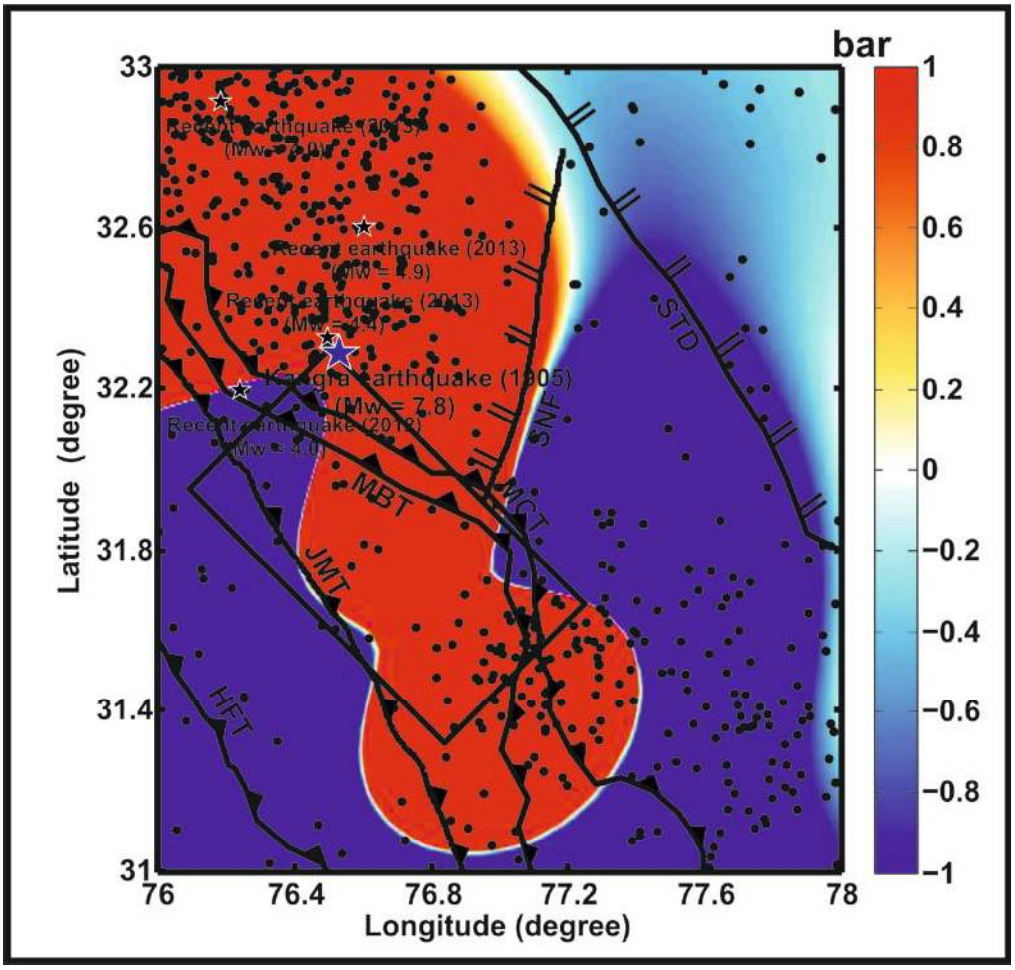

Figure 5.6: clearly demonstrates the high and low stress values over the region due to the occurrence of the 1905 Kangra earthquake with the epicenters of the four recently recorded earthquake events.

5.4.2. 1975 Kinnaur earthquake

The Himalayan orogeny as well-known from the previous studies is the locale to most of the devastating earthquakes in the past. These earthquakes occurring in the region were having their depth of their focus from shallow to intermediate focal depths. On 19 January, 1975, the areas of Kinnaur and Lahaul-Spiti districts, Himachal Pradesh, were rigorously shocked with the occurrence of the magnitude (Ms = 6.8) earthquake (Khattri et al., 1978) as main shock and a number of aftershocks that followed it. As reported earlier by Singh et al., 1975 this earthquake caused an extensive damage to the life and property of the residents for that region. As this earthquake was the major earthquake after the occurrence of the famous great earthquake of 1905 the Kangra earthquake having a magnitude of Ms = 7.8 (Middlemiss, 1910). But the type of faulting associated with the Kinnaur earthquake was different from that of the 1905 Kangra earthquake. This earthquake was characterized by a large component of normal faulting (Banghar, 1975; Khattri et al., 1978) as compared to the 1905 Kangra earthquake which was dominated by the large component of thrust fault mechanism (Middlemiss, 1910). The main shock of 1975 Kinnaur earthquake (mb 6.2 Ms 6.8) occurred at an estimated depth of 33 km (International Seismological Centre, ISC). This part of Himalaya is composed of a number of N–S trending faults that affect the Precambrian-Palaeozoic succession of the Tethys Himalaya of Spiti (Hayden, 1904; Gupta and Virdi, 1975).

The static ΔCFS at the source of the 1975 Kinnaur earthquake is computed first and it is clear from the computation that the rupture propagated along the NNW–SSE direction i.e. the direction of the major structural trends in the Himalaya including the targeted receiver fault (Kaurik-Chango fault). The aftershocks of the earthquake are used in the area as reported by ISC and WIHG catalogue to till date. The aftershocks distributions are well in agreement with the high stress zone. The static ΔCFS is computed at up dip depth of 20 Km with the frictional-coefficient (μ) of 0.40. As most of the aftershocks are having a depth of ~ 20 Km, it is computed at this depth. The focal parameters for the computation at source are having a strike of 163° and dip of 55° adopted from Chaudhary and Srivastva, 1975 for the Kinnaur

earthquake.

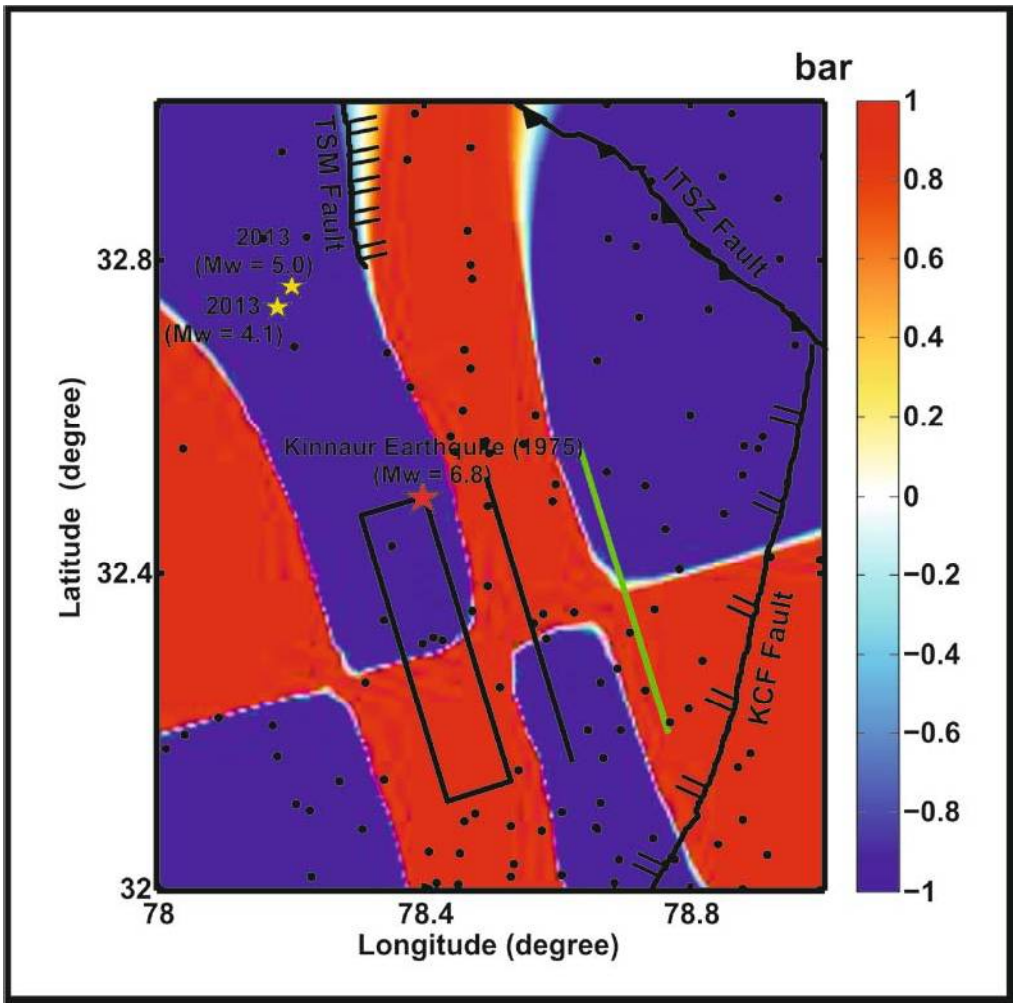

Figure 5.7: ΔCFS computed for 1975 Kinnaur earthquake with the earthquake source acting as major receiver. The aftershocks are plotted as green cross symbol. Major tectonic divisions in the NW Himalaya i.e. Kaurik Fault; ITSZ: Indo Tsangpo suture zone are shown in the map.

But it is unusual to see the Kaurik fault under the stress shadow at that time of the earthquake but now a number of earthquakes in its vicinity show that this fault has been reactivated in the recent years and can be the locale to major earthquakes in future. The two recent earthquakes in the area which also shows normal faulting mechanism having a magnitude of Mw 5.0 and Mw 4.1

can be attributed to the stress imparted by the 1975 Kinnaur earthquake as shown in *Figure 5.7*.

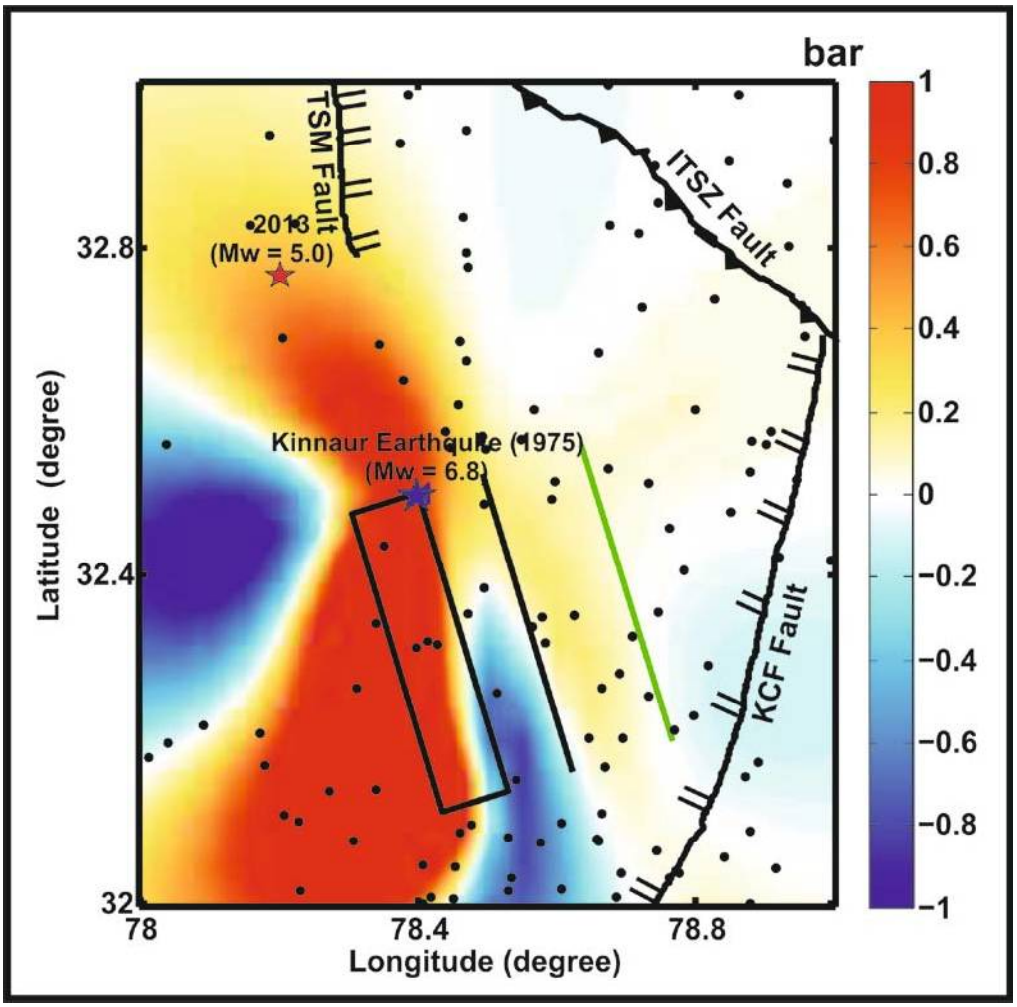

Figure 5.8: ΔCFS computed for 1975 Kinnaur earthquake with the recent earthquake of Mw = 5.0 acting as major receiver. The aftershocks are plotted as green cross symbol. Major tectonic divisions in the NW Himalaya i.e. Kaurik Fault; ITSZ: Indo Tsangpo suture zone; TSM: Tso Morari fault are shown in the map.

These earthquakes are having a strike 207, 324 and dip of 54 and 58 respectively. The dipping of these earthquakes is in well in agreement with the dip of the 1975 Kinnaur earthquake so these earthquakes are well suited as the major aftershocks of the 1975 Kinnaur earthquake. So still the Kinnaur of NW

Himalaya region is under high tectonic stress and can be a home to major earthquake occurrences in future as shown in *Figure 5.8 and Figure 5.9 and Figure 5.10.*

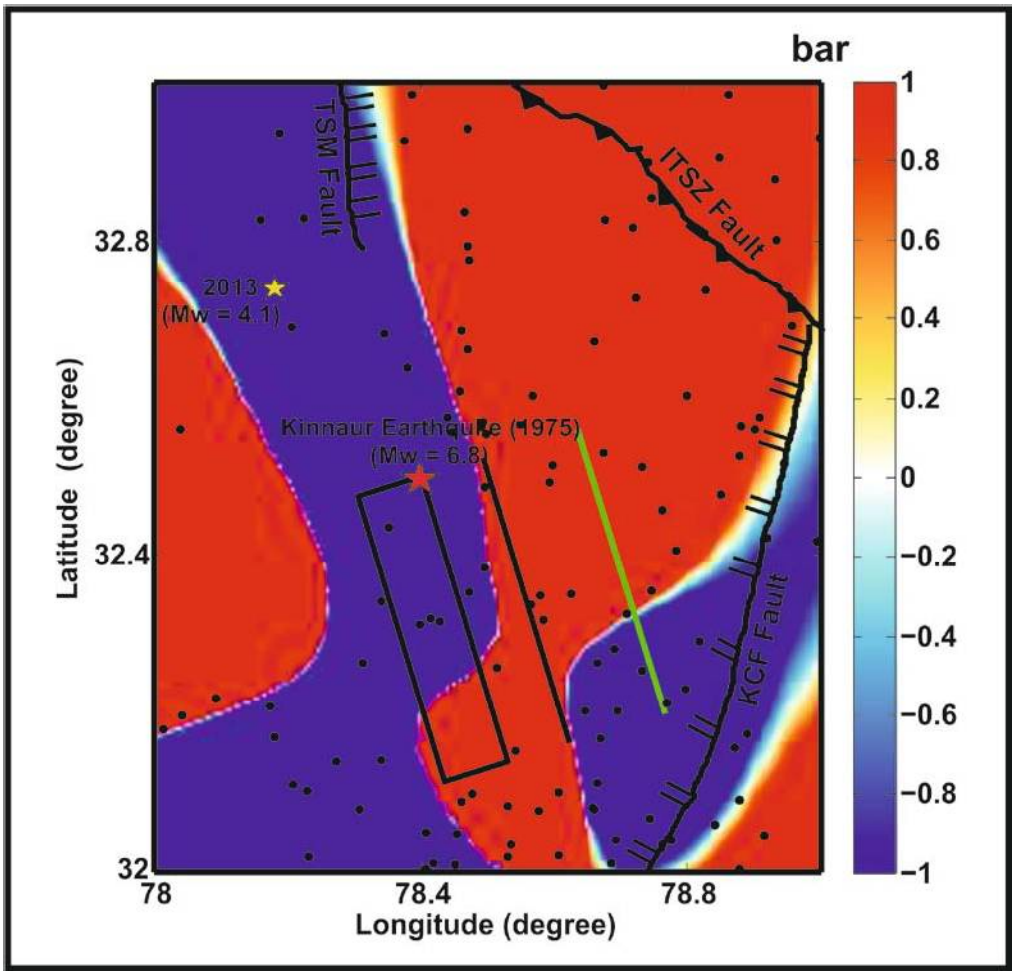

Figure 5.9: ΔCFS computed for 1975 Kinnaur earthquake with the recent earthquake of Mw = 4.1 acting as major receiver. The aftershocks are plotted as green cross symbol. Major tectonic divisions in the NW Himalaya i.e. Kaurik Fault; ITSZ: Indo Tsangpo suture zone; TSM: Tso Morari fault are shown in the map.

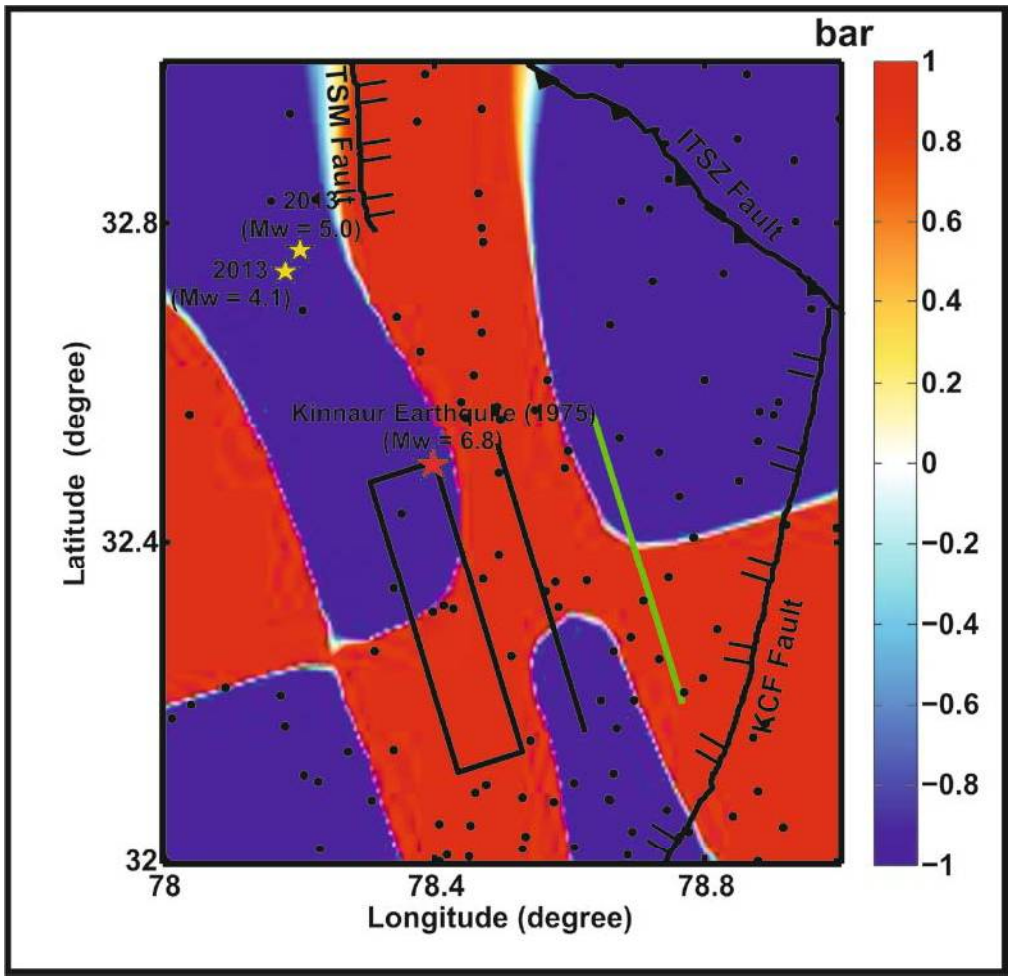

Figure 5.10: ΔCFS computed for 1975 Kinnaur earthquake with the Kaurik fault (secondary fault) acting as major receiver. The aftershocks are plotted as green cross symbol. Major tectonic divisions in the NW Himalaya i.e. Kaurik Fault; ITSZ: Indo Tsangpo suture zone; TSM: Tso Morari fault are shown in the map.

5.4.3. *1991 Uttarkashi earthquake*

The 1991 Uttarkashi earthquake having a magnitude (*Ms* 7.0, *Mw* 6.8, *mb* 6.5) occurred at 30.22°N and 78.24°E in Garhwal-Himalaya of the NW Himalaya region as reported by Centroid moment tensor (CMT) catalogue. This earthquake was regarded to have occurred between the two great earthquakes of the past namely the 1905 Kangra and 1934 Bihar–Nepal earthquake in the central seismic gap. This earthquake resulted due to the tectonic convergence between the India-Eurasia plates. A number of

researchers previously proposed the focal parameters for the earthquake but in the present study focal parameters given by CMT catalogue i.e. strike is about 317°,dip of 14° and slip of 115° is considered. This earthquake is placed to the south of the Main Boundary Thrust (MBT) at a depth of about 15 Km depth. This clearly specifies that the earthquake is placed well above the Main Himalayan detachment (MHT) in the region. This earthquake pertaining to static and dynamic Coulomb stress was calculated by Gupta et al., 2015 and Rajput et al., 2005 but both of the studies failed to prove the stress pertained due to current earthquake on the detachment surface and the future major earthquakes. Gupta et al., 2015 tried to correlate the 1991 Uttarkashi earthquake with the 1999 Chamoli earthquake but from the present analysis it is validated that both the earthquakes are far from being associated with each other. Though the aftershocks of the 1991 Uttarkashi earthquake migrated towards the epicenter of the 1999 Chamoli earthquake but the latter is associated with the Main Central Thrust (MCT) and the former is associated with the continuous tectonic stress loading on the MHT due to the India-Eurasia plate. According to our mentioned phenomena's the static ΔCFS at the source of the 1991 is computed considering the detachment as the major receiver fault and the 2005 earthquake as the major receiver earthquake triggered due to the 1991 Uttarkashi earthquake.

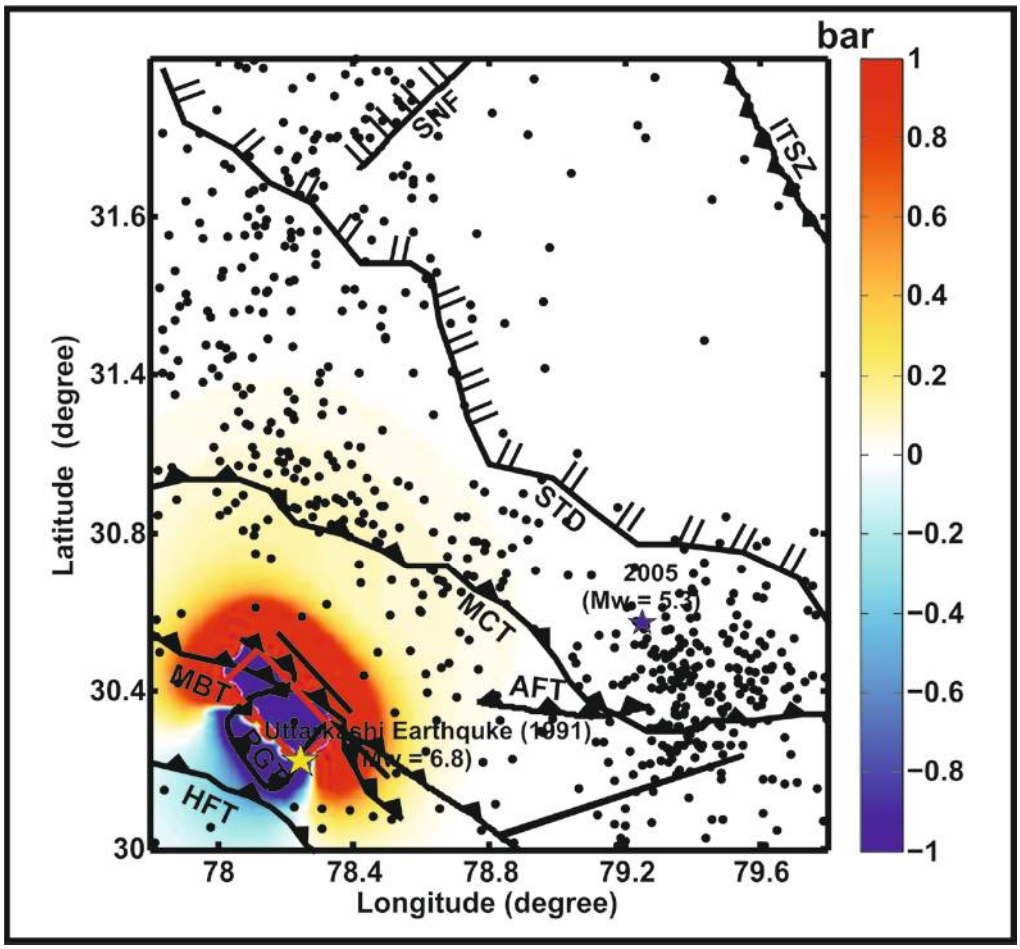

Figure 5.11: ΔCFS computed for 1991Uttarkashi earthquake with the earthquake source acting as major receiver. The aftershocks are plotted as green cross symbol. Major tectonic divisions in the NW Himalaya i.e. HFT: Himalayan frontal Thrust; MBT: Main Boundary Thrust; MCT: Main Central Thrust; STD: South Tibetan Detachment; KCF: Kaurik Chango Fault are shown in the map.

The computation is seen to have a propagation of rupture along the NW–SE direction along the major structural trends including the MHT. The static ΔCFS is computed at a depth of 20 Km and frictional-coefficient of 0.40. The aftershocks which is plotted shows a maximum abundance in the high stress zone propagating along the direction of the rupture and also along the direction orthogonal to the rupture plane. This migration of seismicity towards the epicenter of the 1999 Chamoli earthquake had confused many

researchers that the 1991 Uttarkashi earthquake as a foreshock of the 1999 Chamoli earthquake but it may be suggested that the occurrence of 1999 Chamoli earthquake may be due to the ongoing tectonic convergence of the India-Eurasia plate. Thus latter is not caused due to the stress perturbation of the former. This may have initiated the arrival time of the failure for the 1999 Chamoli earthquake but is not solely responsible for that earthquake occurrence. In the second case the MHT detachment is considered as the receiver for the entire stress perturbed due to the 1991 Uttarkashi earthquake. The focal parameters for the MHT is considered as the Strike of 320°, Dip of 15° and slip of 90° as it is the general trend of the MHT in the region after Molnar 1990. Considering the MHT as the major receiver it can be seen that there is high stress propagating towards the frontal Himalaya though the stress shadow in both the cases remains the same. This shows that the earthquake has significant contribution to the regional tectonic stress field and in future can lead to a number of earthquakes due to the failures of the secondary faults in the region.*Figure 5.12* shows the ΔCFS computed for 1991Uttarkashi earthquake with the MHT (Main Himalayan detachment) detachment acting as major receiver.

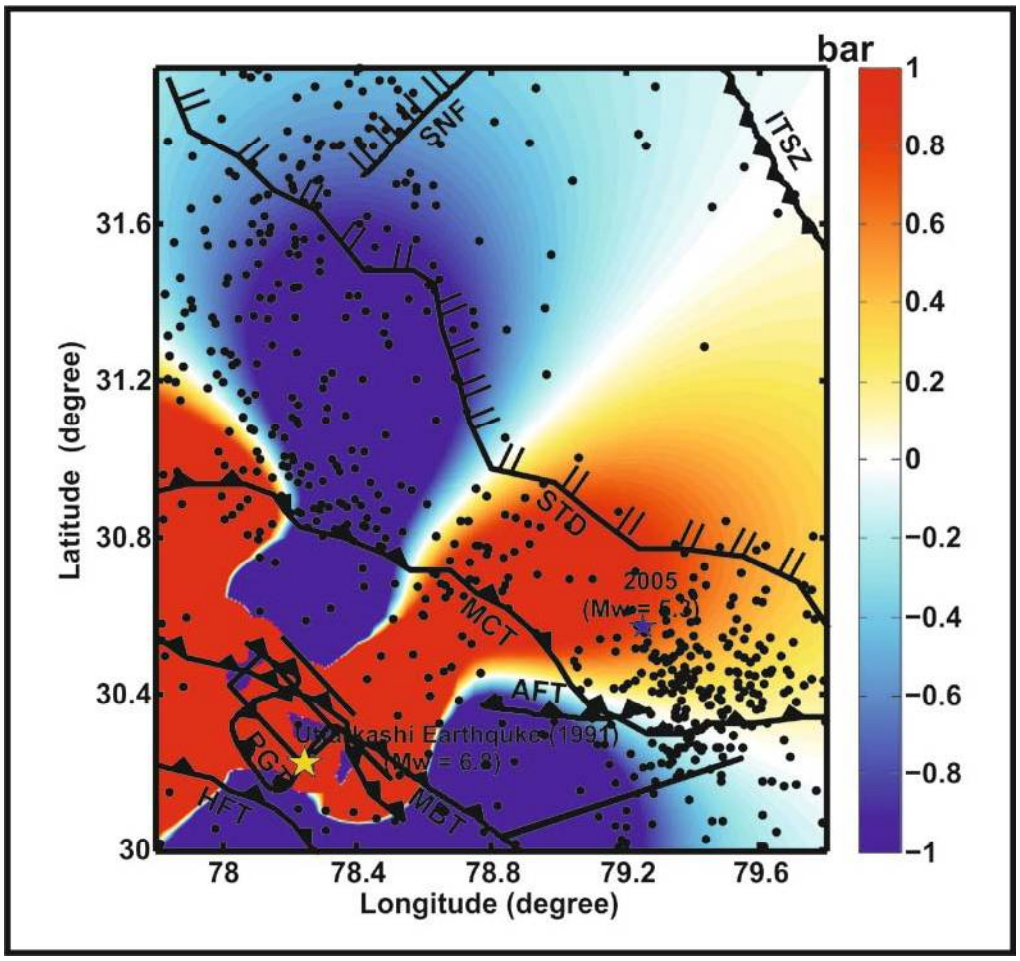

Figure 5.12: ΔCFS computed for 1991Uttarkashi earthquake with the MHT (Main Himalayan detachment) detachment acting as major receiver. The aftershocks are plotted as green cross symbol. Major tectonic divisions in the NW Himalaya i.e. HFT: Himalayan frontal Thrust; MBT: Main Boundary Thrust; MCT: Main Central Thrust; STD: South Tibetan Detachment; KCF: Kaurik Chango Fault are shown in the map.

In the third case the significant earthquake of 2005 in the region as the receiver earthquake is considered. For the static ΔCFS computation, the focal parameters of the earthquake taken as Strike of 293°, Dip of 23° and slip of 86° from the CMT catalogue. The location parameters of this earthquake are 30.48°N and 79.25°E with a focal depth of 44 km. But for the same the ΔCFS at 20 km depth is computed and a frictional-coefficient of 0.40 as it is well known that this earthquake like other earthquakes occurred on the MHT plane

and there may a lot of error in depth computation. It can be seen after computation that there are two stress shadows orthogonal to the Uttarkashi earthquake rupture plane. *Figure 5.13* shows the ΔCFS computed for 1991Uttarkashi earthquake with the recent earthquake of Mw = 5.1 acting as major receiver.

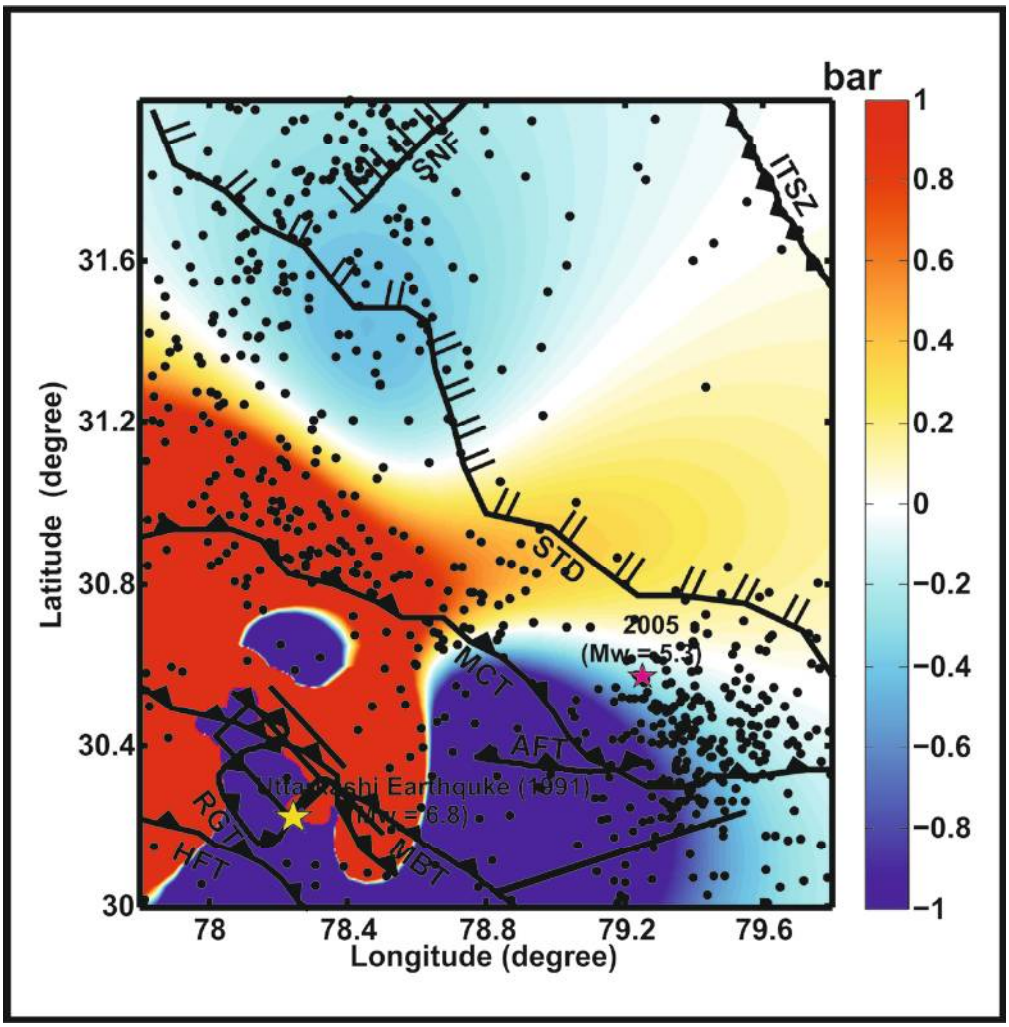

Figure 5.13: ΔCFS computed for 1991Uttarkashi earthquake with the recent earthquake of Mw = 5.1 acting as major receiver. The aftershocks are plotted as green cross symbol. Major tectonic divisions in the NW Himalaya i.e. HFT: Himalayan frontal Thrust; MBT: Main Boundary Thrust; MCT: Main Central Thrust; STD: South Tibetan Detachment; KCF: Kaurik Chango Fault; TSM: Tso Morari fault; SNF: Sundarnager Fault are shown in the map.

It has caused an increased stress in the Higher Himalaya between the MCT and the STD but a significant low in the Tethys Himalaya between STD and the ITSZ also the Kaurik-chango rift or the fault have been placed under stress shadow in the region. Another significant stress shadow can be noted in the lesser and the Siwalik Himalaya over the HFT.

5.4.4. 1999 Chamoli earthquake

On 28th March 1999 a strong earthquake having a reported magnitude of (Ms 6.6, Mw 6.6, and mb 6.3) occurred in the Chamoli region of the Grahwal-Kumaon Himalaya. The epicentre of this earthquake has to be placed at about 100 km southeast of the epicentre of the 1991 Uttarkashi earthquake. The hypocenter parameters reported by the CMT catalogue for the earthquake are 30.38°N latitude and 79.25°E longitude and a focal depth of 15 km. The focal solutions having a strike of 280°, dip of 7° and a rake of 75° as calculated and reported in the Global CMT catalogue is considered. This earthquake occurred at the same depth above the Main Himalayan detachment (MHT) as the 1991 Uttarkashi earthquake. This earthquake is seen to have close proximity with the Main Central Thrust (MCT) that is a steep dipping thrust fault. The grade of metamorphism increases as we move towards MCT with highest grade metamorphic rocks are found within the MCT shear zone. Khattri et al., 1989 had also mentioned the occurrence of moderate earthquakes in the central seismic gap zone due to the reactivation of the low-angle thrust faults in the upper crust parallel to the detachment surface. In case of Chamoli earthquake, the aftershocks were aligned along a direction of the propagation of the rupture. In the view of the much observed analysis of 1999 Chamoli earthquake the static ΔCFS at a depth of 20 Km is computed and frictional-coefficient of 0.40 at the source with the presumed criteria mentioned. The resulted calculation at source depicts that uniform propagation of stress across all directions with a maximum along NE-SW direction almost perpendicular to the rupture of the 1999 Chamoli earthquake. The aftershocks seem to have been concentrated more at tip of the source and also in the close proximity of the Alaknanda fault. *Figure 5.14* shows the ΔCFS computed for 1999 Chamoli earthquake with the earthquake source acting as major receiver.

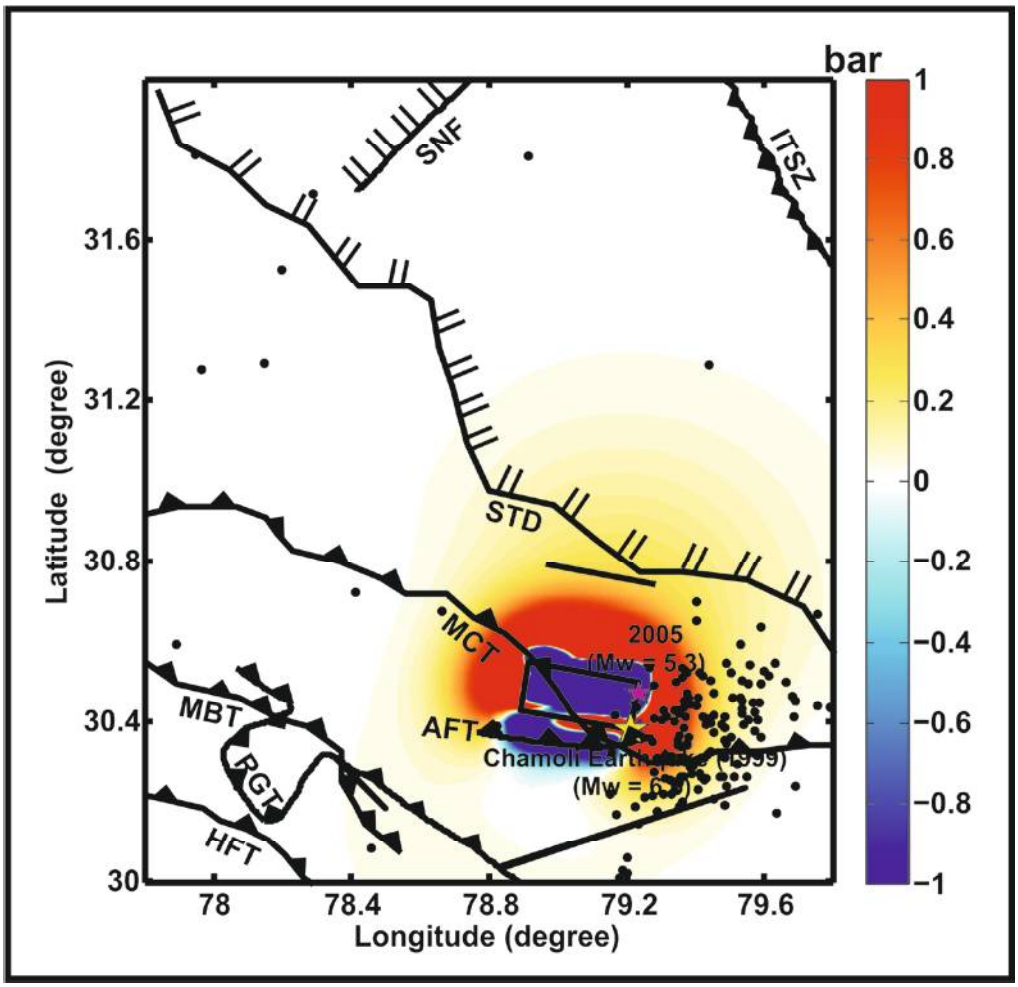

Figure 5.14: ΔCFS computed for 1999Chamoli earthquake with the earthquake source acting as major receiver. The aftershocks are plotted as green cross symbol. Major tectonic divisions in the NW Himalaya i.e. HFT: Himalayan frontal Thrust; MBT: Main Boundary Thrust; MCT: Main Central Thrust; STD: South Tibetan Detachment; Alaknanda Fault are shown in the map.

In the second case the MHT detachment or the basement thrust as the major receiver is considered which consumes the entire seismic stress perturbed due to the 1999 Chamoli earthquake. The detachment is said to have a steep dip in the study area with a dip of 15°, strike of 280° and a rake of 90°. Considering the total transferred stress on to the MHT Plane a high stress shadow perpendicular to the direction of rupture at the source is observed.

The direction of low stress is roughly NE–SW. The high stress is

mainly imparted along the rupture plane that is almost NW-SE. This shows that the earthquake has significant contribution to the regional tectonic stress field and its variation over wide range suggests that in future this can lead to a number of earthquakes due to the failures of the secondary faults in the region.

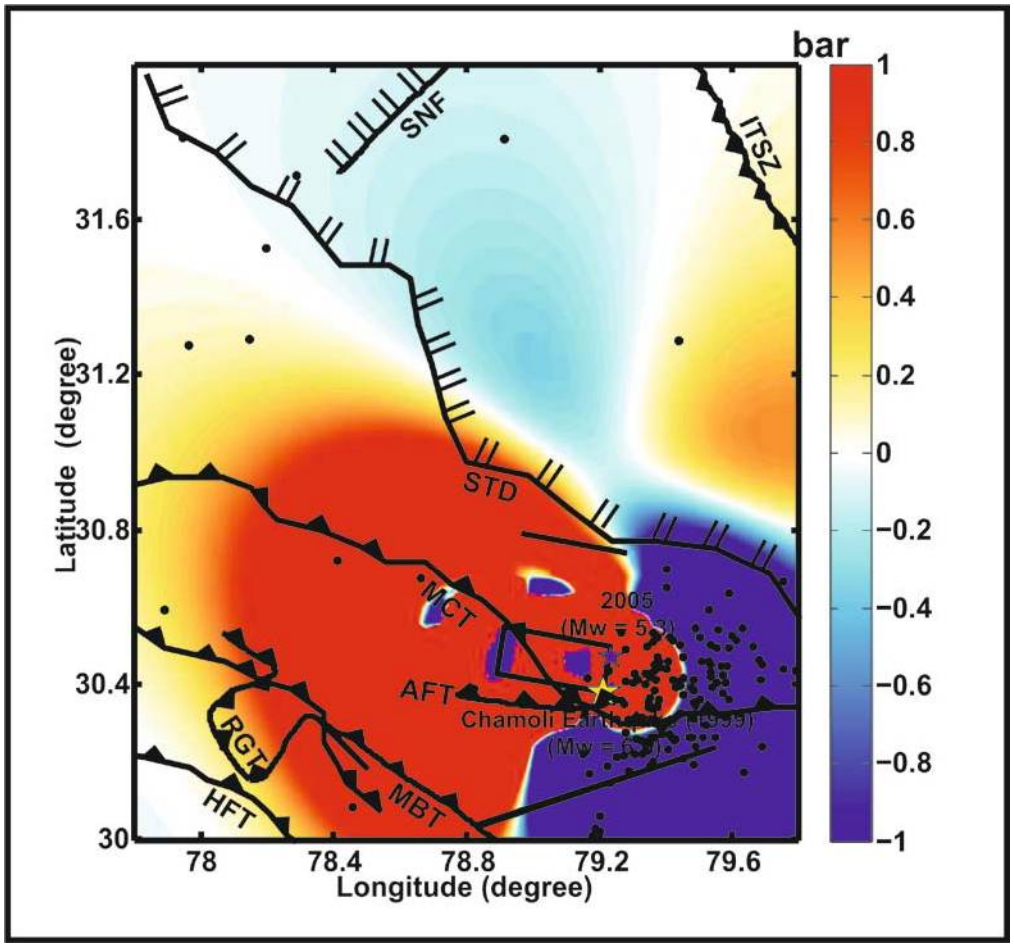

Figure 5.15: ΔCFS computed for 1999Chamoli earthquake with the MHT (Main Himalayan Thrust) acting as major receiver. The aftershocks are plotted as green cross symbol. Major tectonic divisions in the NW Himalaya i.e. HFT: Himalayan frontal Thrust; MBT: Main Boundary Thrust; MCT: Main Central Thrust; STD: South Tibetan Detachment; Alaknanda Fault are shown in the map.

In the third case, the same 2005 significant earthquake occurred near the source region of the 1999 Chamoli earthquake is considered. The

significant earthquake that occurred due to this stress perturbation of the Chamoli earthquake is considered. The static ΔCFS computation is computed for the earthquake with a focal parameters input as Strike of 293°, Dip of 23° and slip of 86° from the CMT catalogue. The location parameters of this earthquake are 30.48°N and 79.25°E with a focal depth of 44 km. The depth of computation is same as it has computed the ΔCFS at 20 km depth and with the same frictional coefficient of 0.40. This earthquake occurred at greater depth but the other earthquakes in the region occurred at shallow depth so there may be significant errors involved in depth computation of the earthquake. It can be seen after the computation that there is a high stress shadow to the south of MCT along the Alaknanda fault. This stress shadow shows a propagating nature in a NW–SE direction along the MBT and is associated with less number of aftershocks. A high stress with larger seismic activity gets aligned along the MCT zone. *Figure 5.16* shows the ΔCFS computed for 1999Chamoli earthquake with the significant earthquake of Mw = 5.1 acting as major receiver.So in broader sense the 1999 Chamoli earthquake has caused a high stress change in Higher and the Tethys Himalaya and resulting in a stress shadow in the lesser Himalaya.

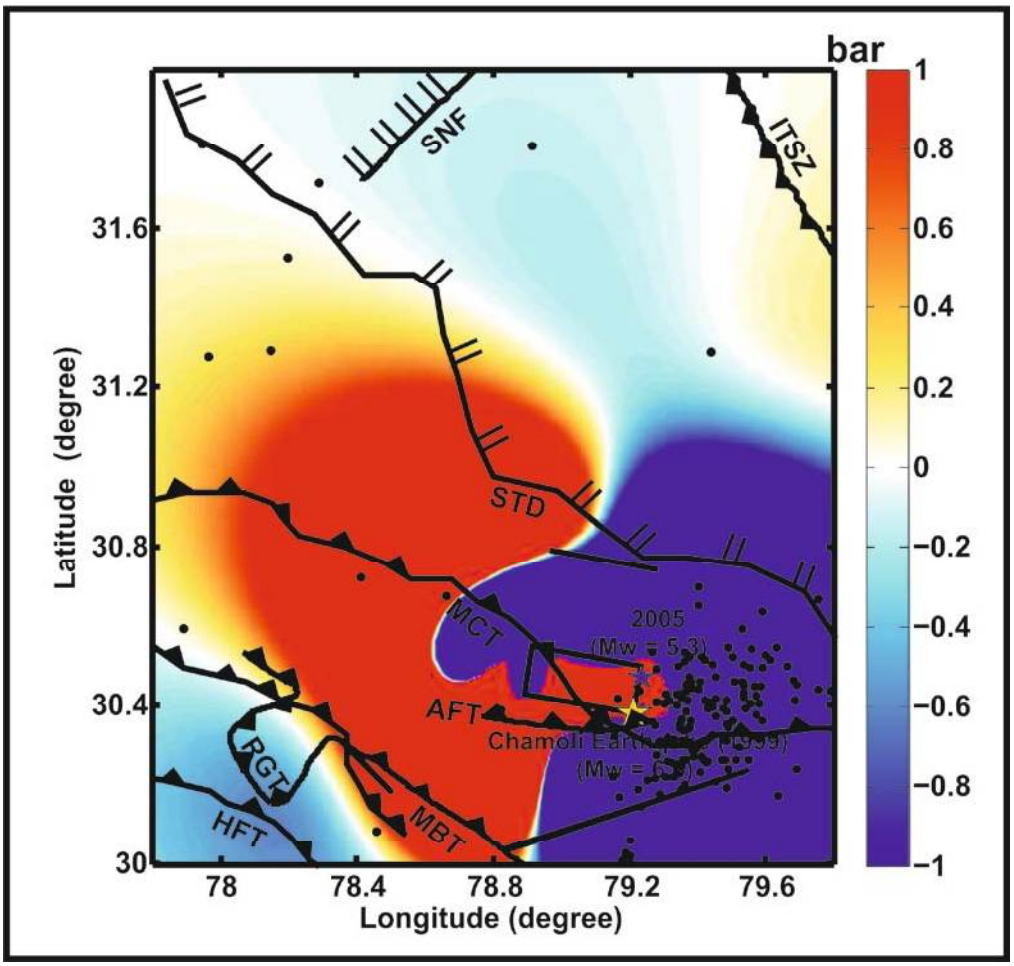

Figure 5.16: ΔCFS computed for 1999Chamoli earthquake with the significant earthquake of Mw = 5.1 acting as major receiver. The aftershocks are plotted as green cross symbol. Major tectonic divisions in the NW Himalaya i.e. HFT: Himalayan frontal Thrust; MBT: Main Boundary Thrust; MCT: Main Central Thrust; STD: South Tibetan Detachment; Alaknanda Fault are shown in the map.

Therefore, the present study pertaining to the stress pattern scenario shows how the stress is varying across major structural provinces of the NW Himalaya region after the occurrences of the major earthquakes in the past.